

**Surface modified CFx cathode material for ultrafast discharge and high energy density**

Journal:	<i>Journal of Materials Chemistry A</i>
Manuscript ID:	TA-ART-10-2014-005492
Article Type:	Paper
Date Submitted by the Author:	14-Oct-2014
Complete List of Authors:	Dai, Yang; Shanghai institute of space power sources, Cai, Sendan; Shanghai Institute of Space Power Sources, Wu, Lijun; Brookhaven national lab., Yang, Weijing; Shanghai institute of space power sources, Xie, Jingying; Shanghai Institute of Space Power Sources, Wen, Wen; Shanghai Synchrotron Radiation Facility, Shanghai Institute of Applied Physics, Chinese Academy of Science, Zheng, Jin-Cheng; Xiamen University , Department of Physics Zhu, Yimej; Brookhaven National Laboratory,

Surface modified CF_x cathode material for ultrafast discharge and high energy density

Yang Dai^{1,6+}, *Sendan Cai*¹⁺, *Lijun Wu*³, *Weijing Yang*¹, *Jingying Xie*^{1,5**}, *Wen Wen*⁴,
Jin-Cheng Zheng^{2*}, and *Yimei Zhu*^{3*}

¹Shanghai Institute of Space Power Sources, Shanghai 200245, China

²Department of Physics, and Fujian Provincial Key Laboratory of Theoretical and Computational Chemistry, Xiamen University, Xiamen 361005, China

³Condensed Matter Physics & Materials Science Department, Brookhaven National Laboratory, Upton, New York 11973, United States

⁴BL14B1 Shanghai Synchrotron Radiation Facility, Shanghai, 201204, China

⁵Shanghai Engineering Center for Power and Energy Storage Systems, Shanghai 200245, China

⁶Department of Chemical Engineering School of Environmental and Chemical Engineering, Shanghai University, Shangda Road 99, Shanghai, 200444, China

⁺ Yang Dai and Sendan Cai contributed equally to this work

ABSTRACT

* Address to corresponding authors: J. X. (Jyxie@mail.sim.ac.cn), J. Z. (jczheng@xmu.edu.cn) and Y. Z. (zhu@bnl.gov)

Li/CF_x primary possesses the highest energy density of 2180Wh/kg among all primary lithium batteries. However, a key limitation for its utility of this type of batteries is its poor rate capability because the cathode material, CF_x, is intrinsically a poor electronic conductor. Here, we report on our development on a controlled process of surface de-fluorination under mild hydrothermal condition to modify the highly fluorinated CF_x. The modified CF_x, consisting of an in-situ generated shell component of F-graphene layers, possesses good electronic conductivity and removes the transporting barrier for lithium ions, yielding a high-capacity performance and excellent rate-capability. Indeed, a capacity of 500 mAh/g and a maximum power density of 44800 W/kg can be realized at ultrafast rate of 30 C (24A/g), that is over one-order-of-magnitude higher than that of the state-of-the-art primary lithium-ion batteries.

KEYWORDS: *primary lithium batteries; carbon fluoride; de-fluorination; ultrafast discharge*

Introduction

The Li/CF_x primary battery is the first lithium battery developed since 1970's,¹ and possesses the highest energy-density among all primary lithium batteries (theoretically 2180Wh/kg). In critical environment, such as deep underground or those far afield, in tire-pressure monitoring systems, and in space exploration, the cutting-edge CF_x chemical system offers a long service-life, high reliability, a wide range of operating temperature and demonstrated excellent electrochemical performances that is not achievable by the common lithium or so-called beyond

lithium-systems (such as lithium-sulfur batteries, lithium-air batteries, sodium-sulfur batteries, and so on) systems.²⁻⁴ However, the Li/CF_x battery is known to suffer from kinetic problems due to the intrinsically poor electronic conductivity of the cathode material CF_x, inhibiting its applications in high-power devices.^{5 - 8} Considerable efforts have been devoted to addressing these problems. Various nanoscale carbon materials, such as carbon nano-fibers,⁹ carbon nanotubes, fullerenes,⁸ and ordered meso-porous carbon,¹⁰ were fluorinated by various methods to improve their electrochemical performances. And an impressive 8057 W/kg power density (6C) associated with a capacity of 440 mAh/g was achieved in fluorinated carbon fibers.⁹ Other approaches were devoted to modifying the CF_x materials. Generally, researchers usually applied the “doing addition” methods to achieve the modification, such as polypyrrole coating,⁷ carbon-thermal treatment,^{11, 12} and grapheme/SVO ball milling. However, the rate capability remained limited. And the CF_x reported in literature so far failed to realize a discharge rate over 10C. Unfortunately, the CF_x cathode also exhibits a low capacity at high rates (termed “low Faradic yield”), so compromising the energy density. Thus, the challenge is on how to design and prepare the CF_x material that possesses high rate capability without trading off energy density.⁵

In this paper, we report an alternative “doing subtraction” approach to modify highly fluorinated CF_x. We realize it by applying a controlled surface de-fluorination process under mild hydrothermal conditions. During defluorination, an electrical conductive surface is generated and the barriers to ion transport are removed. Once,

the limitation on electron transfer and ion transport at the electrode level is removed, the innate rate capability of CF_x is revealed to be very high. We demonstrated that, even the CF_x can also achieve an ultrahigh power-density of 48800W/kg at 30 C, with a capacity of 500 mAh/g. The electrochemical performances, especially the rate capability are significantly improved compared to those of the state-of-the-art.

Experimental Section

Modification of CF_x . Modified CF_x was synthesized by a simple hydrothermal reaction between precursor CF_x (Daikin corp. Graphite precursor, $x=1.17$) and base water/ethanol mixed solution. In a typical procedure, an NaOH (0.72g) and $\text{CH}_3\text{CH}_2\text{OH}$ /water mixture (90mL, 50/50 wt%) was blended by ultra-sonication for 1 min. Then, the mixture was transferred into a 150mL Teflon-lined autoclave and maintained at 180°C for 8 h. Afterwards, the autoclave was naturally cooled to room temperature, and the product was subsequently filtered through a microporous membrane and washed throughout with ultrapure water. Finally, the modified CF_x was obtained by vacuum drying at 60°C for 24 hours. If not specially mentioned, the modified CF_x is assigned to be treated using this procedure. The C/F ratios of the CF_x were determined by a chemical method and carried out in Shanghai Institute of Organic Chemistry, Chinese Academy of Science (CAS).

Material Characterization. The surface morphologies of the CF_x were visualized by scanning electron microscopy (SEM) using a Hitachi S4800 microscope. HRTEM, atomically resolved scanning transmission electron microscopy (STEM) and electron

energy loss spectroscopy (EELS) experiments were performed using the JEOL aberration-corrected transmission electron microscope (JEM-ARM200F) at Brookhaven National Laboratory. The microscope was equipped with a cold-field emission source and a Gatan Quantum ER energy filter. Under normal operating conditions, a probe size of 0.1 nm with a 0.5eV energy resolution is routinely achieved. The structure of the samples was characterized by synchrotron radiation X-ray diffraction (XRD), using the BL14B1 beamline at the Shanghai Synchrotron Radiation Facility (SSRF) and the wavelength of the X-ray employed is $\lambda = 1.2398 \text{ \AA}$. BL14B1 is a bending magnet beamline, and the storage ring energy of SSRF is 3.5 GeV. The beam was first collimated using a Rh/Si mirror and then monochromatized using a Si(111) double-crystal monochromator. After that, the beam was further focused by a Rh/Si mirror to the size of $0.5 \text{ mm} \times 0.5 \text{ mm}$. Higher-order harmonics were also rejected by the Rh/Si mirror. A NaI scintillation detector was used for data collection. X-ray photoelectron spectroscopy (XPS) was performed using a RBD upgraded PHI-5000C ESCA system (Perkin Elmer). A Shirley-type background was removed from the spectra before de-convolution.

Electrode Fabrication. CF_x (80 wt%) powder, PVDF resin (10 wt%, Kynar 761), and vapor grown carbon fiber (VGCF, 10%, Showa Denko Co.) were mixed and stirred vigorously in the presence of N-methyl-2-pyrrolidone to form a uniform slurry. The cathodes were prepared by spreading the same slurry onto carbon coated aluminum foil (18 μm) current collectors. The thickness of the composite active layers is set around 25 μm after drying and rolling depression. Then coated Al foil was

punched into disks of 1.4 cm in diameter, of which, the active mass loading were about 2 mg. The theoretical capacity of the CF_x was calculated using $Q = xF/[3.6(12+19x)]$ (where x is the fluorine content, F is the Faraday constant 96.485C/mol and 3.6 is the conversion constant¹²).

First principles calculations. First principles calculations were carried out using the WIEN2k code¹³ with the method of full potential linearized augmented plane wave plus local orbital (FP-LAPW+lo). The exchange-correlation interaction is described by the Perdew-Burke-Ernzerh of generalized gradient approximation (PBE-GGA).¹⁴ The muffin-tin radii are selected as 1.25 a.u. for C, and 1.30 a.u. for F. The k-points of 15x15x2 for Brillouin zone sampling are used in the calculations. The EELS images are obtained by TELNES2 package in the WIEN2k code.

Results

Material synthesis and structural characteristics. Although highly fluorinated CF_x is hard to de-fluorinate at low temperature, it is still easy to react with NaOH in an H_2O/CH_3CH_2OH solution, even at a lower temperature (180 °C) under hydrothermal conditions. In this study, CH_3CH_2OH played a paramount role, serving as the co-solvent and the “surfactant” to wet the CF_x powder. From the optical photograph (Figure 1 (a)), the color of the pristine material is light gray, indicating the precursor graphite has been highly fluorinated. During the hydrothermal process (Figure 1 (e) and (f)), the C-F bond on the surface of the pristine CF_x is activated to form a new shell, leaving F^- in the solution. Thus, the color of modified CF_x turns shiny black (Figure 1 (b)), with F content decreasing from 62 to 58.7 wt%. This

reduction of surface F content also affects the contrast quality of the SEM images (Figure 1 (c) and (d)). Figure 1 (c) shows the typical layer stacking structure and the morphology of pristine CF_x with a particle size of about several to twenty micrometers, indicating the CF_x is generated from the graphite-like precursor. The blurred edges of the pristine particles point to their poor conductivity. In comparison, the SEM image of the modified one is clear, revealing the superior electron conductivity after hydrothermal treatment. In addition, the morphology of the modified particle exhibits more cracks, shaped like those in weathered granite. This might be induced by being “struck” by alkali ions under the high temperature and pressure conditions.

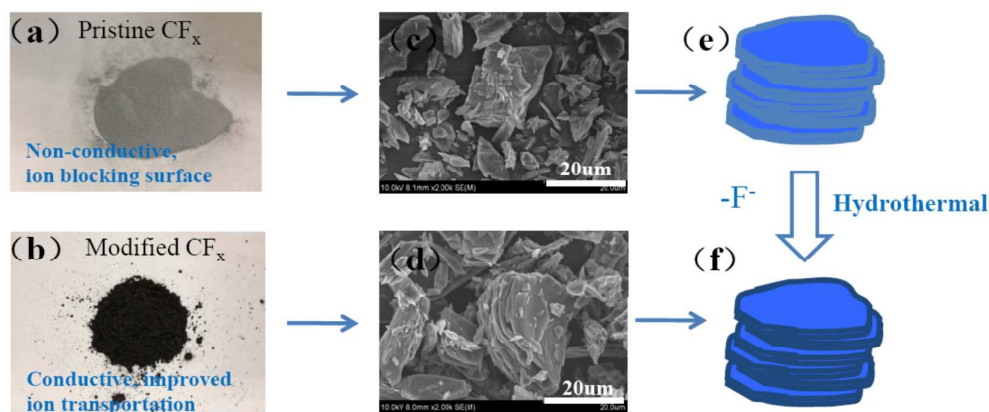


Figure 1. The optical micrographs and SEM images of the pristine (a) and modified CF_x powders (b). Conductivity difference in the two materials is visible from the SEM images, as is blur for the pristine (c) but much more clearer for the modified one (d). The light edge around the particles refers to the high F-containing moieties such as $-\text{CF}_2$ or $-\text{CF}_3$ groups in pristine CF_x (e). The dark edge around the modified particles (f) indicates the in-situ de-fluorinated layers, which possess higher carbon content.

The synchrotron x-ray diffraction pattern (Figure S2) of the pristine CF_x shows typical broad peaks corresponding to the fluorinated phases (radiation wave length:

0.124nm), with $2\theta \approx 10^\circ$, 20.4° and 32.6° assigned, respectively, to the CF_x (002) (referred as P_1 below), graphite (002) (referred as P_2) and graphite (100) (referred as P_3) peaks. It appears that the position and shape of the diffraction peaks do not change after the modification, implying that the de-fluorination process does not affect the major structure of the particles.⁷ However, a close inspection, especially a quantitative fitting of the peaks, reveals that the intensities ratio of the P_2/P_1 and P_3/P_1 increase from 0.11 to 0.17, 0.11 to 0.2 after modification, indicating an increase in graphite structure.

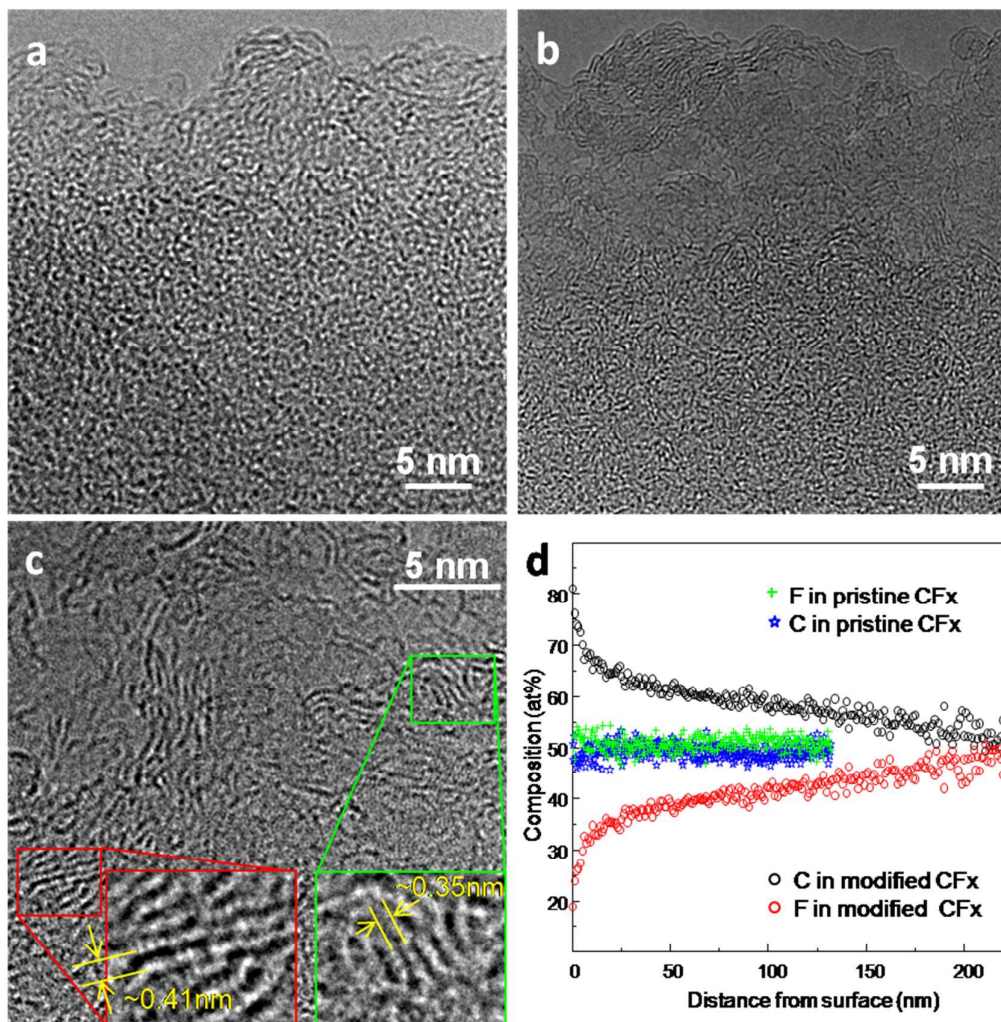


Figure 2 (a-c) High resolution TEM (HRTEM) images taken from (a) pristine CF_x, and (b,c) modified CF_x particles. (d) the composition of C and F as a function of distance from the surface for pristine and modified CF_x (calculated from the EELS spectrum image in Figure S1).

To understand how the structure changes after modification, we carried out structural analysis using high resolution transmission electron microscopy (HRTEM). Figure 2 shows the HRTEM images taken from pristine CF_x (Figure 2a), and modified CF_x particles (Figure 2b, 2c). The pristine CF_x presents irregular atomic arrangement, which is common in highly fluorinated CF_x.¹⁵ Inside the particle, e.g. in the bottom of (a) and (b), the modified CF_x has basically the same amorphous structure as the

pristine CF_x . However, on the surface, e.g. top part of (a) and (b), the modified CF_x presents fringes like graphite or diamond polytypes,^{16, 17} while the pristine CF_x still exhibits an irregular atomic arrangement. These results indicate the graphite and diamond polytypes are the major structure on the surface region (up to several tens of nanometers) in the modified CF_x . To further confirm the structural changes on the surface of the modified CF_x , we carried out EELS spectrum image analysis in scanning transmission electron microscopy (STEM) mode in our double aberration corrected microscope (for details, see Fig. S1). Figure 2d shows the composition of C and F as a function of distance from the surface for pristine and modified CF_x calculated from the EELS spectrum image in Fig. S1. While the compositions of C and F are constant for pristine CF_x , the F concentration decreases from the interior of the particle to the surface. In the surface region (~ 15 nm), the concentration of F drops considerably. The results clearly show that the surface of the modified CF_x particle is de-fluorinated and also the rearrangement of the F-graphene layers (sp^2 or sp^3 carbon rearrangement), while the core is basically unchanged, echoing the overall decrease of CF_x structure (or the increase of graphite) revealed by XRD. Raman spectra of different CF_x are depicted in Figure S3 and a pair of peaks is observed around 1340 cm^{-1} (D-band) and 1580 cm^{-1} (G-band). However, the why and how such chemical gradient is produced along the microstructure are really hard to explain at this time. We will work on this in the future. The intensity ratio of the D and G bands (I_D/I_G), is known to depend on the number of defects within the CF_x (the disorder-induced band). The I_D/I_G ratio of pristine CF_x is 1.39, thus confirming the

presence of C-F sp^3 hybridized carbon atoms.¹⁸ On the other hand, the defect ratio for the modified CF_x ($I_D/I_G = 1.85$) is higher, indicating the increase in defect concentration after de-fluorination. As will be discussed later, the superior electrochemical performance of modified CF_x can be attributed to the advantageous features offered by its unique microstructure.

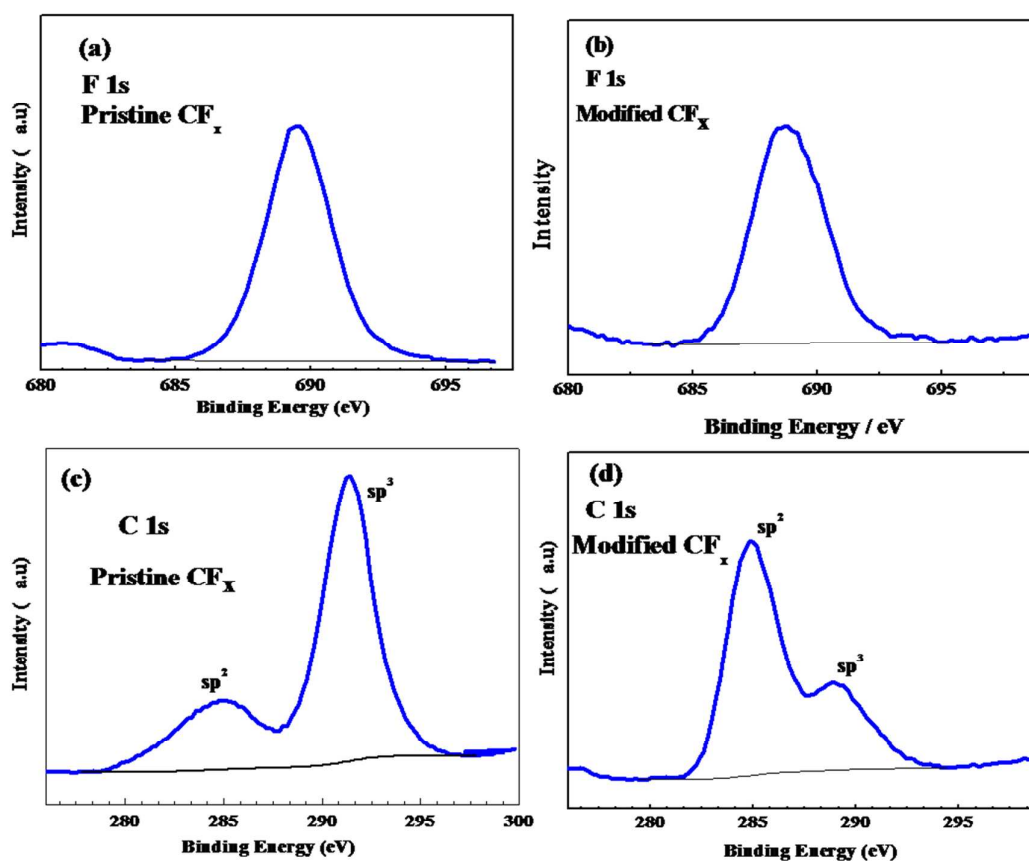


Figure 3. X-ray photoelectron spectroscopy spectrum of F1s for (a) pristine and (b) modified CF_x ; and C1s for (c) pristine and (d) modified CF_x . (b) shows a small red shift of about 1.0 eV in comparison with (a).

The surface structure change can be further analyzed by surface-sensitive X-ray photoelectron spectroscopy (XPS). From the F1s XPS spectrum in Figure 3a, a

characteristic peak is found at 689.8 eV in pristine CF_x corresponding to the covalent F species that exists in highly fluorinated carbon.⁹ In comparison, a small shift about 1.0 eV is evident in Figure 3b, revealing a change in the chemical environment for F atoms after de-fluorination. The F 1s peak in semi-ionic and ionic C-F bonds are located at 688.2 eV and 685.9 eV respectively¹⁰ from which we speculate that after modification, parts of the covalent C-F bonds are transformed into semi-ionic ones, which is reasonable for lower F content moieties (C/F=1.5) (see detailed XPS peak fittings and assignments in Figure S4 and Table S1). As shown in Figures 3c and d, the C 1s of pristine and modified CF_x , two components of C-containing (284.6 eV for $C=C<$, sp^2 hybridization) and the F-containing moieties (sp^3 hybridization, associated with the $-CF_2$ and $-CF_3$ groups) are exhibited.¹⁵ The normalized peak area ratio of F-containing and C-containing moieties for pristine CF_x is estimated at 2.47 while a dramatic decrease of about 2 is represented in the modified CF_x , i.e. 0.44. Moreover, the difference between the sp^3 and sp^2 hybridization peaks for pristine and modified CF_x reduced from 6.5 eV to 4.0 eV, which may be due to the formation of lower F content species, such as $C-C(CF_3)_3$ (288.2 eV) and $FC(C)_3$ (289.2 eV) after de-fluorination,¹⁰ corresponding to diamond-like and graphite-like polytypes found by HRTEM, as shown in Fig. 2(c). In fact, for the highly fluorinated CF_x , high F content species such as $F_2C(CF_3)_2$ (located at 291.0 eV) and $F_2C(CF_2)_2$ (291.8 eV) groups are likely to be generated on the edge of sheets and at the defects in the precursor surface.^{5,10} On the contrary, the bonding energy range for those high F content groups can hardly be found in modified CF_x (Figure 3d). In addition,

compared to the pristine CF_x , the peak area ratio of C-containing to F-containing for modified CF_x is greatly enhanced (from 0.86 to 1.52). This increase could be attributed to the de-fluorination and rearrangement of the carbon atom to form $\text{C}=\underline{\text{C}}<$ bonds during the hydrothermal process.

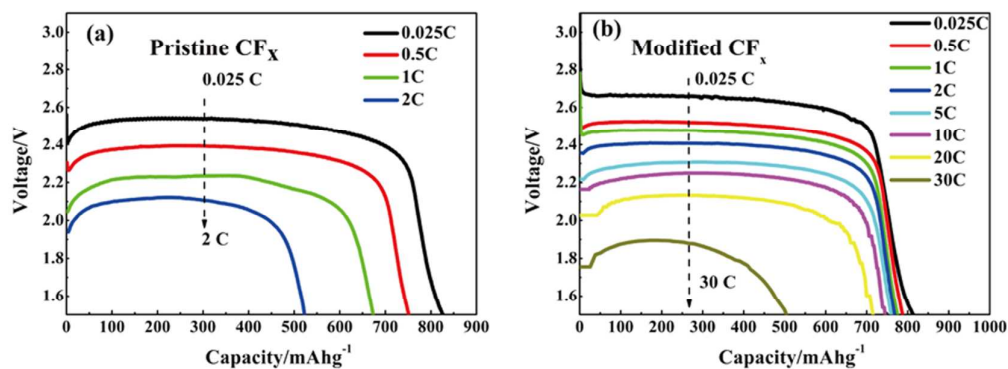


Figure 4 Discharge profiles of (a) pristine and (b) modified CF_x . The voltage delay phenomenon is eliminated for the modified CF_x at the rate of 0.025C.

Electrochemical performances. Coin cells (2016) with a metallic Li counter electrode were used to evaluate the electrochemical performance of materials (Figure 4a, b). The pristine composite cathode delivers a discharge capacity of 825 mAh/g (theoretical value 916 mAh/g, $\text{CF}_{1.17}$) at 0.025 C, with a plateau of 2.5V. A voltage delay is obviously seen from the curve. Although using an optimized conducting network (VGCF 10 wt %) ¹⁰ and a stress relief current collector (carbon coated Al foil) ^{15, 16}, the pristine CF_x still shows poor electrochemical performance at the discharge rate of 2C, with a capacity of only 520 mAh/g. The modified CF_x cathode ($x = 0.89$ estimated according to the F content of 58.7 wt%) exerts a capacity of 820 mAh/g at 0.025C, close to the theoretical capacity (825 mAh/g). More interestingly,

the discharge plateau rises to 2.65V without any voltage delay, verifying the good electronic and ionic conductivity of the active particles at the initial stage of discharge.^{5,8} Whereas CF_x cathodes are known to suffer from sluggish kinetics, our modified CF_x electrodes demonstrated outstanding high rate capability. The specific capacity of the modified CF_x composite cathodes at the fast discharge rates of 5C and 20C is 757 and 715 mAh/g, respectively, which is impressively 92 % and 87 % of that at 0.025 C. Even at the ultrafast rate of 30 C (24 A/g), a significant high capacity of 500 mAh/g and a maximum power density of 48400 W/kg (based on the active material) still can be obtained. Clearly, despite of the large particle size (SEM images in Figure 2), lithium ions can still rapidly reach the inside of the active material. We also investigated the CF_x treated with different NaOH equivalents (0.36 g, and 2.88 g). Compared to the pristine samples, the rate performances were improved. The material treated with 0.72 g NaOH showed the best performance.

Discussion

It is well known that the good electronic and ionic conduction is expected to contribute to high capacity and high rate capability. During the high fluorination process of pristine CF_x , the $-\text{CF}_2$ and $-\text{CF}_3$, which are considered as inactive groups hindering the lithium ion diffusion, are likely to be generated on the surface.⁵ This would cause surface electronic insulation and ionic traffic blocking, leading to poor faradic yield and rate capability. In contrast, after de-fluorination, the surface inactive groups are eliminated, and rearrangements occur to form a more electronic conductive

surface (see HREM results in Figure 2 and XPS results in Figure 3). The increase of electronic conductivity of CF_x after de-fluorination is supported by first principles all-electron calculations.

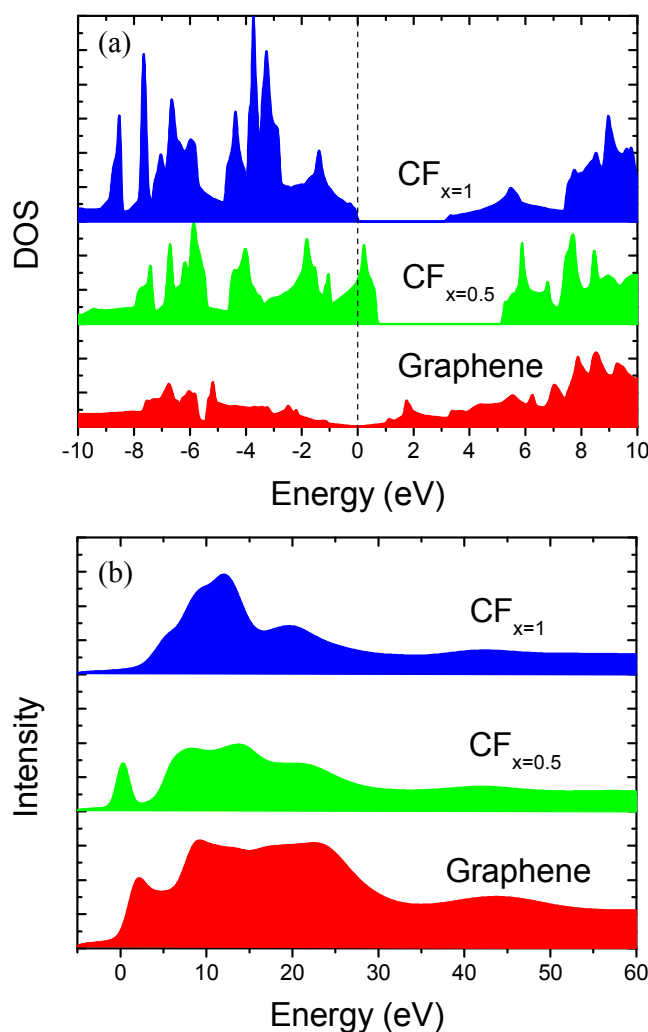


Figure 5 Density of states (DOS) (a) and EELS (b) of CF_x obtained by first principles all-electron calculations based on density functional theory. The Fermi energy is indicated by dashed line in (a). Fully fluorinated carbon, CF_x ($x=1$), shows wide band gap. However, for CF_x ($x=0.5$), it shows metallic like feature, as indicated by the high DOS at the Fermi level. The present of separated and significant prepeak in EELS (b) for CF_x ($x=0.5$) comparing with CF_x ($x=1$) is a signature of de-fluorination, which is in good agreement with experimental measurement (see Fig. S1).

As shown in Figure 5, the fully fluorinated CF_x with an $x=1$ sheet presents wide-band-gap characteristics, while for de-fluorinated one such as CF_x with $x = 0.5$, a metallic-like feature is observed. As shown in the schematic illustration (Figure 6), the conductive surface can lower the resistance for electron transfer and provide more electronic paths to form effective conducting-network in the electrode.

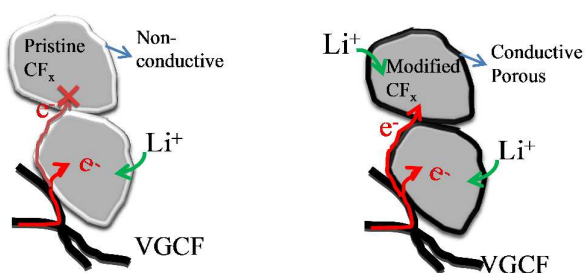


Figure 6 Schematic diagram of electronic paths for pristine and modified CF_x during discharge. The light edge around the particles in the left part of the figure refers to the high F-containing moieties such as $-\text{CF}_2$ or $-\text{CF}_3$ groups in pristine CF_x . While the dark lines around the modified particles indicates the in-situ defluorinated layers, which possess high carbon content.

More importantly, the traffic for ion transport is improved since surface inactive groups such as $-\text{CF}_2$ and $-\text{CF}_3$ have been removed during de-fluorination. As shown in previous reports on CF_x modification,⁵⁻¹¹ researchers have been devoted to the electron transfer, but overlooked the ion transport problems of CF_x . Although the electronic conductivity is enhanced, the ion transport barriers (such as $-\text{CF}_2$, $-\text{CF}_3$), or ion transport paths disruption during the modification still exist. Thus, it was hard to achieve high rate capability ($>10\text{C}$) and high faradic yield. In this study, graphite-like and diamond-like carbon domains formed in the outer layer generating porous

structure could provide abundant channels without any barriers for lithium-ion transport (Figure 2c).^{19, 20} Once the limitations are removed, high capacity and ultrafast rate performances can be achieved. To better understand our findings, an analysis of electrochemical impedance spectrum (EIS) at the open circuit voltage (OCV) was performed (see Figure S6). Clearly, the cell reaction resistance (R_c , the semicircles) of the modified CF_x are only about half that of the pristine one, revealing the low resistance and improved conductivity. The onset between the semicircle and the sloped line are indicative of reaction kinetics with higher frequencies representing faster reaction kinetics, which indicates primarily a low reaction resistance.¹¹ Therefore, the EIS measurements corroborated the effective promotion of electron and ion transfer by the modified CF_x electrode.

Conclusions

In conclusion, we have developed a simple and effective de-fluorination method to modify CF_x cathodes through a hydrothermal process. The modified CF_x , consisting of an in-situ generated shell component of F-graphene layers, possesses good electronic conductivity deprived of transporting barriers of $-CF_2$, $-CF_3$ groups for lithium ions. Thus, high capacity performance and excellent rate capability without capacity compromising can be obtained. A capacity of 500 mAh/g and a maximum power density of 48400 W/kg are realized at ultrafast rate of 30C (24A/g). Our findings demonstrate a new route to achieving high power density CF_x material. More importantly, the promising utilities for high-power, high energy and long service life

using the modified CF_x material are exciting, particularly for application in launchers for space exploration and in life-saving medical devices.

Acknowledgements

Financial support from the National Natural Science Foundation of China (No. 21103109, No.21373137, No.U1232110), and Shanghai Science and Technology Talent Program (No. 12XD1421900) are greatly appreciated. The specialized research fund for the doctoral program of higher education (No. 20100121120026). The work at Brookhaven National Laboratory is supported by the U.S. Department of Energy, Office of Basic Energy Sciences, under Contract No. DE-AC02-98CH10886.

Supporting Information.

This material is available free of charge via the Internet at <http://pubs.acs.org>.

References

- (1) Watanabe, N.; Fukuda, M. US Patent 3,536,532 (1970) and 3,700,502 (1972).
- (2) Watanabe, N.; Nakajima, T.; Touhara, H. *Graphite Fluorides*, Elsevier, Amsterdam, **1988**.
- (3) Hamwi, A.; Guerin, K.; Dubois, M.; *Fluorinated Materials for Energy Conversion*, Elsevier, Oxford, UK, **2005**.
- (4) Bruce, P.; Freunberger, S.; Hardwick, L.; Tarascon, J. M. *Nature Materials*. **2012**, *11*, 19-29.
- (5) Guerin, K., Dubois, M.; Houdayer, A.; Hamwi, A. *J. Fluorine Chem.* **2012**, *134*, 11.
- (6) Meduri, P.; Chen, H.; Chen, X.; Xiao, J.; Gross, M.; Carlson, T.; Zhang, J.; Deng, Z. *Electrochem. Commun.* **2011**, *13*, 1344.
- (7) Groult, H.; Julien, C.M.; Bahloul, A.; Leclerc, S.; Briot, E.; Mauger, A. *Electrochem. Commun.* **2011**, *13*, 1074.
- (8) Dubois, M.; Guérina, K.; Zhang, W.; Ahmad, Y.; Hamwi, A.; Fawal, Z.; Kharbache, H.; Masin, F. *Electrochimica Acta* **2012**, *59*, 485.
- (9) Lam, P.; Yazami, R. *J. Power Sources* **2006**, *153*, 354.
- (10) Fulvio, P.; Brown, S.; Adcock, J.; Mayes, R.; Guo, B.; Sun, X.; Mahurin, S.; Veith, G.; Dai, S. *Chem. Mater.* **2011**, *23*, 4420.
- (11) Zhang, S.; Foster, D.; Read, J. *J. Power Sources*, **2009**, *188*, 601.
- (12) Zhang, Q.; Astorg, S. D.; Xiao, P.; Zhang, X.; Lu, L. *J. Power Sources* **2010**, *195*, 2914.

- (13) Blaha, P.; Schwarz, K.; Madsen, G. K. H.; Kvasnicka, D.; Luitz. *Schwarz (Vienna University of Technology, Austria, 2001)*, **2001**.
- (14) Perdew, J. P.; Burke, K.; Ernzerhof, M.; *Phys. Rev. Lett.*, **1996**, *77*, 3865.
- (15) Wang, Z.; Wang, J.; Li, Z.; Gong, P.; Liu, X.; Zhang, L.; Ren, J.; Wang, H.; Yang, S. *Carbon*, **2012**, *50*, 5403.
- (16) Ownby P.D.; Yang, X.; Liu, J. *J. Am. Ceram. Soc.* **1992**, *75(7)*, 1876.
- (17) Spear, K. E.; Phelps, A. W.; White, W. B. *J. Mater. Res.*, **1990**, *5(11)*, 2277.
- (18) Sato, Y.; Ootsubo, M.; Yamamoto, G.; Lier, G.; Terrones, M.; Hashiguchi, S.; Kimura, H.; Okubo, A.; Motomiya, K.; Jeyadevan, B.; Hashida, T.; Tohji, K.; *ACS nano* **2008**, *2*, 348.
- (19) Brezesinski, T. ; Wang, J.; Tolbert , S.; Dunn, B. *Nature materials*, **2011**, *9*, 146.
- (20) Magasinski, A.; Dixon, P.; Hertzberg, B.; Kvit, A.; Ayala, J.; Yushin, G. *Nature materials* , **2010**, *9*, 353.

TOC

A simple and effective de-fluorination method is developed to modify CF_x cathodes through a hydrothermal process that greatly improves the capacity performance and rate capability of CF_x by removal of surface ionic transport barriers. A capacity of 500 mAh/g and a maximum power density of 48400 W/kg was achieved at an ultrafast rate of 30C (24A/g).

Surface modified CF_x cathode material for ultrafast discharge and high energy density

TOC figure

